Biosensors and Bioelectronics 127 (2019) 108–117

Contents lists available at ScienceDirect

Biosensors and Bioelectronics

journal homepage: www.elsevier.com/locate/bios

A novel photosensitive dual-sensor for simultaneous detection of nucleic acids and small chemical molecules

Jing Wang[a,b,c,d], Xun Cui[a,e], Jingyu Zhu[f,g], Luxi Tan[a,d,*], Lichun Dong[a,d,*]

[a] School of Chemistry and Chemical Engineering, Chongqing University, Chongqing 400044, PR China
[b] College of Chemistry and Molecular Engineering, Peking University, Beijing 100871, PR China
[c] School of Chemical and Biomolecular Engineering, Georgia Institute of Technology, Atlanta 30332, USA
[d] Key Laboratory of Low-grade Energy Utilization Technologies & Systems of the Ministry of Education, Chongqing University, Chongqing 40004, PR China
[e] School of Materials Science and Engineering, Georgia Institute of Technology, Atlanta, GA 30332, USA
[f] School of Life Science, Sichuan University, Chengdu 610041, PR China
[g] State Key Laboratory of Biotherapy & Cancer Center, West China Hospital, Sichuan University & National Collaborative Innovation Center, Chengdu 610041, PR China

ARTICLE INFO

Keywords:
DNA nanotechnology
Dual-sensor
DNA melting
Gene expression
Nucleic acids

ABSTRACT

Sensors that can rapidly and specifically detect nucleic acids and chemical molecules can revolutionize the diagnosis and treatment of diseases by allowing molecular-level informations to be used during the routine medicines. In this study, we demonstrated a novel dual-sensor that can be used to simultaneously detect any nucleic acids and chemical molecules whose binding aptamers can be found or synthesized. In the developed dual-sensor, the specifically designed PTG (a photosensitive azobenzene derivative carrying one photo-isomerizable azobenzene moiety, one threoninol terminal and one guanidinium terminal) molecules are introduced into the unwinding region of two T7 promoters, and two DNA bubbles are introduced upstream of the two T7 promoters. Without the target, the indicating gene in the dual-tensor would not be expressed since the binding with RNAPs (RNA polymerases) cannot melt the T7 promoter for the indicating gene due to the integration of the DNA double strands *via* the PTG molecules, manifesting the absence of the target nucleic acid and chemical molecule. While with the presence of the target nucleic acid and/or chemical molecule, the indicating gene would be expressed as the T7 promoter contained in the enlarged DNA bubble can be melted and transcribed by the bound RNAPs as the enlarged DNA bubble can help the separation of the two DNA strands, demonstrating the existence of target nucleic acid and/or chemical molecule.

1. Introduction

With the recent technological development, nucleic acid detecting and chemical assaying are becoming important clinical tools for implementing personalized medicines, effective diagnosis of infectious diseases as well as cancer management (Lee et al., 2010; Cho et al., 2009; Mairal et al., 2008; Banga et al., 2014; Smith et al., 2017; Despras et al., 2016). The most commonly used sensors for detecting nucleic acids are southern blots and combinatorial DNA chips, which rely on the specific hybridization of the surface-bound single-strand capture oligonucleotides to the complementary targets; however, the sensitivity of the two detection systems, decided by the dissociation properties of the capture strands hybridized to perfect and to mismatched complements (Elghanian et al., 1997; Mirkin et al., 1996), is unsatisfactory due to the low concentration of the target nucleic acids in cells and circulating blood. Another major challenge for the sensitive and selective detection of nucleic acids is the small size (usually 18–24 bp) of some tiny nucleic acids, which requires the design of short primers for the classic PCR (polymerase chain reaction), leading to the reduction of detection efficiency and increase of the nonspecific amplification at the same time (Duan et al., 2013; Koshiol et al., 2010; Leshkowitz et al., 2013; Harcourt and Kool, 2012). Recently, the nanoparticle-based detection systems for nucleic acids have received more and more attentions due to the multiple advantages (Ge et al., 2014; Munge et al., 2005; Gao et al., 2012; Soleymani et al., 2011, 2009): the large surface-to-volume ratio, the versatile structures and tunable physical properties, and the molecular-scale curvature on the surfaces of nanoparticles that can enhance the display of probe molecules (Smith et al., 2017; Taton et al., 2000). However, the nanoparticle-based nucleic acid detecting systems are complex and costly. As the chemical assaying, the spectroscopic and chromatographic techniques have been demonstrated to be effective for detecting small molecules (Tagliaro et al.,

* Corresponding authors at: School of Chemistry and Chemical Engineering, Chongqing University, Chongqing 400044, PR China.
E-mail addresses: tanluxi@cqu.edu.cn (L. Tan), lcdong72@cqu.edu.cn (L. Dong).

https://doi.org/10.1016/j.bios.2018.12.015
Received 30 October 2018; Received in revised form 3 December 2018; Accepted 7 December 2018
Available online 13 December 2018
0956-5663/

1994; Trachta et al., 2004; Buryakov, 2004; Strano-Rossi et al., 2005), while these methods are cumbersome, and moreover, the accompanying reduction of the affinity between the target and the detection system could gradually decrease the detection sensitivity (Baker et al., 2006).

It has been well demonstrated that sensors employing aptamers that reassemble in the presence of targets can achieve excellent sensitivity for detecting small chemical molecules with a variety of advantages (McKeague and DeRosa, 2012; Ruigrok et al., 2011; Jayasena, 1999; Mok and Li, 2008; Stojanovic et al., 2001; Yang et al., 2014). Firstly, aptamers can be chemically synthesized with high reproducibility at a relatively low cost; second, DNA aptamers can be used under harsh conditions and stored with a long shelf life due to their excellent chemical stability; finally, it is able to generate unstructured aptamers that can form specific secondary structures such as three-way junctions or tertiary folds upon binding with targets, demonstrating the existence of targets. However, the target-induced conformational change of aptamers is hard to control, *e.g.* some small-molecule-binding aptamers may have relatively high dissociation constants (McKeague and DeRosa, 2012); some well-characterized target-binding aptamers are structurally stable, forming three-way junctions even before binding with targets (Stojanovic et al., 2001), which leads to unreliable detections.

All the above-mentioned strategies for nucleic acid detecting and chemical assaying are based on the structural changes of DNA (conformational change, hybridization and melting of DNA) (Elghanian et al., 1997; Mirkin et al., 1996; Ge et al., 2014; Munge et al., 2005; Gao et al., 2012; Soleymani et al., 2011, 2009; McKeague and DeRosa, 2012; Stojanovic et al., 2001); however, few studies in the literatures have tried to initiatively regulate the structural changes of DNA for nucleic acid detecting and chemical assaying although the strategy has been widely used for controlling gene expression. Asanuma et al. (1999a, 1999b) realized the clear-cut regulation of the formation and dissociation of DNA duplex by introducing an azobenzene derivative into the DNA backbone *via* a three-carbon-atom linker. Ultraviolet (310–370 nm) or visible light (> 400 nm) could induce a reversible isomerization between the *trans* and *cis* conformation of the introduced azobenzene derivative. When the azobenzene derivative is in the *cis* conformation, the two strands of the double-standard DNA are forced to depart from each other, leading to the dissociation of DNA duplex. Liu et al. (2006) also proposed a strategy for photo-controlling the transcription of the target gene *via* the T7 RNA polymerase by introducing azobenzene molecules into the side chain of the T7 promoter. Wang et al. (2017a) reported an approach to enhance the expression of target genes by introducing a DNA bubble in the promoter region of DNA duplex through the binding of the DNA aptamers with the corresponding ligands. Bergen et al. (2016) introduced a new and generic tool for photo reversible assembly of DNA nanostructures relying on the addition of an azobenzene-containing guanidinium molecules that can non-covalently interact with the unmodified DNA and affect its melting temperature under light irradiation.

Among the various DNA structural changes, DNA hybridization/melting is a key step in multiple biotechnological processes, *e.g.* DNA amplification by PCR, DNA repair and enzyme synthesis (VanGuilder et al., 2008; Wilhelm and Pingoud, 2003; Niemeyer et al., 1999), accordingly, the regulation of DNA hybridization/melting provides a convenient approach for controlling gene expression, which paves the basis for the rapidly developing DNA nanotechnology (Seeman, 2003; Rothemund, 2006; Sacca and Niemeyer, 2012; Niemeyer, 2000; Krishnan and Simmel, 2011; Nykypanchuk et al., 2008). In this study, we developed a novel dual-sensor relying on the regulation of DNA hybridization/melting that can be potentially used for cost-effectively detecting and quantifying two targets (one nucleic acid and one small chemical molecule) at the same time *via* the expression and non-expression of two indicating genes (*rfp* gene and *gfp* gene). When the tested system does not contain any target, none of the indicating genes can be expressed; while when the tested system contains one target, the corresponding gene can be expressed. Moreover, when the tested system contains both the targets, both of the indicating genes can be expressed, and the concentration of the fluorescent proteins (RFP, red fluorescence protein, encoded by *rfp* gene; GFP, green fluorescence protein, encoded by *gfp* gene) can be measured to quantify the corresponding targets. The advantage for the dual-sensor to detect and quantify the target nucleic acid and small chemical molecule at the same time is: when the test system mutates or is infected with a virus, especially the system from human body, the system would produce some nucleic acids and the related small chemical molecules. When using the developed dual-sensor to detect the target nucleic acid and chemical molecule, the dual-sensor can distinguish whether the chemical is produced by the test system by verifying the coexistence of the target nucleic acid and chemical molecule, or due to the contamination by the foreign chemical *via* manifesting the existence of only the target chemical molecule, or the test system has potential to produce the target chemical *via* manifesting the existence of only the target nucleic acid.

2. Material and methods

Materials and Methods is available in the Supporting information; PTG (a photosensitive azobenzene derivative carrying one photoisomerizable azobenzene moiety, one threoninol terminal and one guanidinium terminal) Synthesis (Scheme S1); Synthesis of the modified DNAs involving PTGs (Scheme S2); Optimum DBnaDAP and DBctDAP for the dual-sensor (Figs. S1 and S2); The configurations of PTG molecule under visible light or dark condition. (Fig. S3); Effectiveness of the proposed dual-sensor under the dark condition. When the number of PTGs introduced in the unwinding region is between 2 and 5 (the maximum number of PTGs can be introduced into the unwinding region is 5), the dual-sensor can operate effectively; when the number is less than 2, the dual-sensor is not effective (Fig. S4); Effect of PTGs introduced in the unwinding region on the RNAPs (RNA polymerases) to recognize and melt the promoter under the dark condition with/without the target (Fig. S5); Effects of PTGs introduced in both the recognition region and unwinding region on the K_m, k_{cat} values and the RFP/GFP concentration of the *rfp/gfp* gene under the dark condition or UV irradiation at 365 nm with/without the target (Tables S1-S4); Effectiveness of the proposed dual-sensor under the dark condition (a. DS-02-D) and under the UV irradiation at 365 nm (b. DS-54-UV). A: RFP concentration when only 50 aM of Oligo was added 2; B: GFP concentration when only 50 aM of Oligo 2 was added; C: RFP concentration when only 1.2 μM of thrombin was added; D: GFP concentration when only 1.2 μM of thrombin was added; E: RFP concentration when both 50 aM of Oligo 2 and 1.2 μM of thrombin were added; F: GFP concentration when both 50 aM of Oligo 2 and 1.2 μM of thrombin were added (Fig. S6); Sequences of the dual-sensor (Fig. S7; **Fragment A**, **Fragment B** and **Fragment C**).

3. Results and discussion

3.1. The working mechanism of the developed dual-sensor

The key of the dual-sensor developed in this study is to control the expression of the indicating genes by regulating the melting of the promoter DNA. In the dual-sensor, two DNA bubbles are introduced upstream the two T7 promoters for encoding the two indicating genes (*rfp* gene for indicating the nucleic acid and *gfp* gene for indicating the target chemical molecule). Among the two DNA bubbles, the DNA bubble for the *rfp* gene (naDNA bubble, the distance between the naDNA bubble and the T7 promoter (DBnaDAP) = 0 bp) is induced due to the non-complementary state of the ssDNA sequences in the sense and antisense strands of the double-stranded DNA that can hybridize with the target nucleic acid; while the DNA bubble for the *gfp* gene (ctDNA bubble, the distance between the ctDNA bubble and the T7

promoter (DBctDAP) = 12 bp) is induced due to the non-complementary state of the DNA aptamer (Iyer and Doktycz, 2014) that can be bound by the target chemical molecule (the optimum DBnaDAP and DBctDAP have been studied in Figs. S1 and S2 of the Supporting information). The hybridization of the target nucleic acid with the ssDNA sequence would lead to the enlargement of the naDNA bubble around the ssDNA in the local structure of the double-stranded DNA for accommodating the target nucleic acid, while the binding of the target chemical molecule with the ctDNA bubble would lead to the enlargement of the ctDNA bubble (Wang et al., 2017a, 2017b). Moreover, in the developed dual-sensor, a number of PTG (a photosensitive azobenzene derivative carrying one photoisomerizable azobenzene moiety, one threoninol terminal and one guanidinium terminal, Schemes S1 and S2) molecules are specifically designed and introduced into the unwinding region of the double-stranded DNA. The PTG molecules form covalent bonds with the three-carbon-atom linker in one strand of DNA *via* the threoninol terminal (Asanuma et al., 1999), and interact non-covalently with the other strand due to the high affinity of the DNA phosphate groups towards the PTG guanidinium terminal (Blondeau et al., 2007; VanGuilder et al., 2008), resulting in the integration of the two DNA strands (Fig. 1). For the cases that the PTG molecules are not introduced, the indicating genes would be expressed regardless of the existence or inexistence of the target as the RNA polymerases (RNAPs) can bind and melt the T7 promoter as usual. But when sufficient PTG molecules are introduced, the indicating gene would not be expressed without the target since the binding with RNAPs cannot melt the T7 promoter due to the integration of the DNA double strands *via* the PTG molecules (Fig. 1a). While with the presence of the target, the enlarged DNA bubble would help to break the non-covalent interaction between the PTG molecules with the single DNA strand, leading to the separation of the two DNA strands, consequently, the T7 promoter for the indicating gene contained in the enlarged DNA bubble can be melted and transcribed by the bound RNAPs (Weisburg et al., 1991), the resulted expression of the indicating gene would manifest the existence of the corresponding target (Fig. 1b). The developed dual-sensor can detect any nucleic acids and a significant number of chemical molecules whose binding aptamers can be found or synthesized as long as their concentration exceeds a very low value (about 10 ppm) that they can

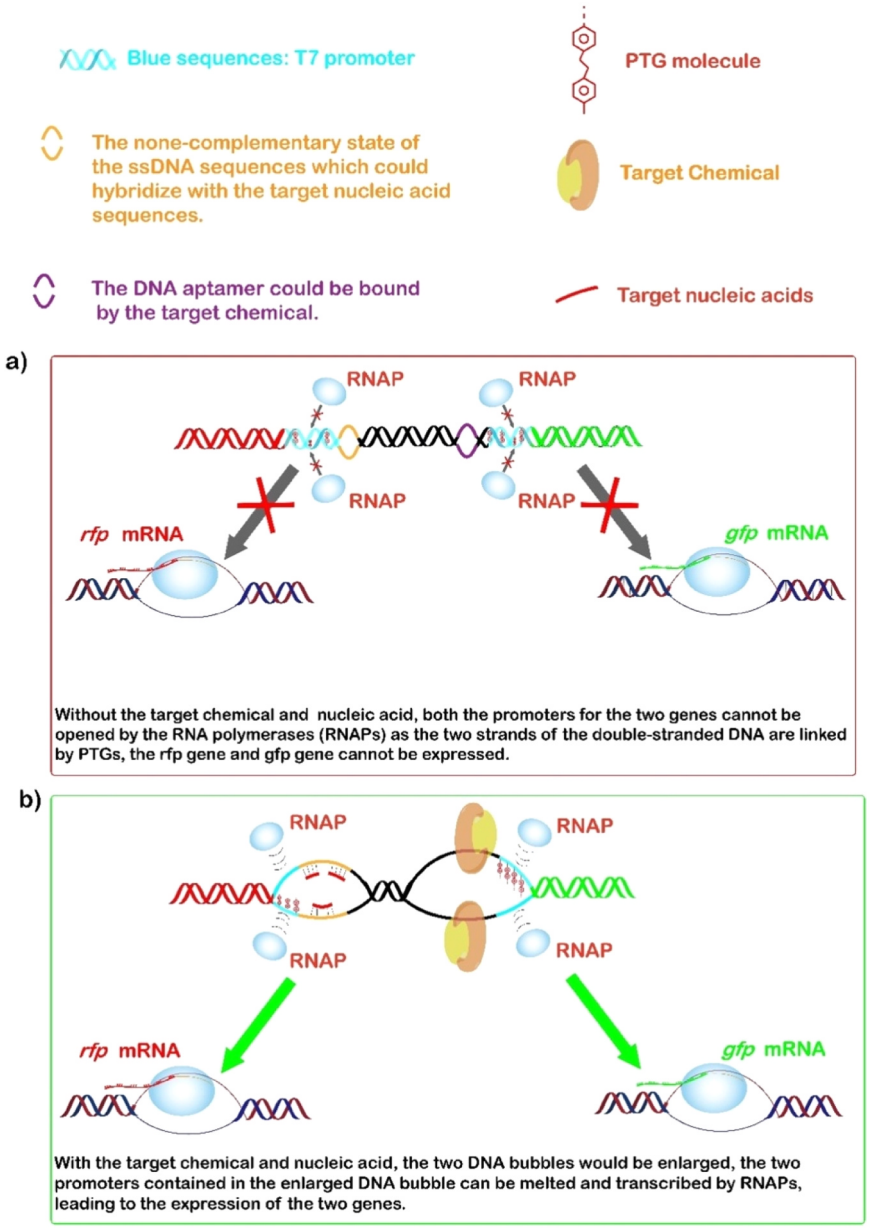

Fig. 1. The working mechanism of the dual-sensor without (a) or with (b) the target.

hybridize with the specific nucleic acid sequence and aptamer contained in the DNA bubbles.

3.2. Effectiveness of the proposed dual-sensor

Under the visible light or dark condition, PTG molecules are in the *trans* configuration, indicated by the intense and broad characteristic absorption band around 357 nm (π-π*) in the UV–Vis absorption spectrum (Fig. S3) (Beharry and Woolley, 2011; Merino and Ribagorda, 2012). While under UV irradiation (at 365 nm, 0.35 mW cm^{-2}), a *trans-cis* isomerization would occur for the PTG molecules, indicated by the disappearance of the absorption peak at 357 nm and two emerging bands, *i.e.* a less intense band around 319 nm (π-π*) and a broad band around 440 nm (n-π*) in the UV–Vis absorption spectrum (Beharry and Woolley, 2011; Merino and Ribagorda, 2012). The *trans-cis* isomerization of PTG molecules leads to the weakened non-covalent interaction between the PTG molecules with the single strand of the double-stranded DNA and hydrogen bonds between the two stands of the double-stranded DNA. Therefore, the effect of the introduced *trans*-PTG molecules on the affinity between the two stands is different from that of the introduced *cis*-PTG molecules, which is verified by measuring the melting temperature (T_m) of the T7 promoter double-stranded DNA as well as a 15 bp double-stranded oligonucleotide (Oligo 1). The DNA thermal denaturation have been studied to test the T_m of the DNA temples according to Bergen's method (Bergen et al., 2016). The results in Fig. 2a showed that T_m of the T7 promoter DNA increases dramatically from 23 °C to 39 °C as 6 PTG molecules were introduced, while after a short time of UV irradiation at 365 nm, the melting curve of the T7 promoter DNA significantly shifts toward the lower temperatures with the melting temperature decreasing from 39 °C to 31 °C. Similar results were also observed for Oligo1 introduced with 6 PTG molecules, T_m increases from 18 °C to 34 °C after the PTG molecules were introduced, while decreasing to 25 °C after UV irradiation (Fig. 2b).

Once sufficient PTG molecules are introduced in the unwinding region of the double-stranded DNA, the bound RNAPs cannot melt the T7 promoter without the help of the enlarged DNA bubble (Weisburg et al., 1991). Consequently, without the target, the indicating gene in the dual-tensor would not be expressed, manifesting the absence of the target nucleic acid and chemical molecule. While with the presence of the target nucleic acid and/or chemical molecule, the indicating gene would be expressed as the enlarged DNA bubble can help the separation of the two DNA strands (Wang et al., 2017a; Weisburg et al., 1991), demonstrating the existence of target nucleic acid and/or chemical molecule. Moreover, the results in Figs. S4 and S5 and Tables S1 and S2 demonstrated that under dark condition, the dual-sensor is not effective when only one PTG molecule is introduced in the unwinding region, at this scenario, the binding of RNAPs with T7 promoter can break the non-covalent interaction between the PTG molecule with the single DNA strand without the help of the enlarged DNA bubble, resulting in the expression of the *rfp* gene and *gfp* gene whether the target is present or absent (Wang et al., 2017a, 2017b). For the same reason, under UV irradiation, the dual-sensors are effective only when the PTG molecules introduced in the unwinding region are 4 or 5 (Fig. 3). Moreover, Fig. 4b shows that compared with the case that 5 PTG molecules are introduced in the unwinding region, a smaller K_m value (meaning faster recognition of the T7 promoter by RNAP) and a larger k_{cat} value (meaning faster unwinding of the promoter) would be obtained when 4 PTG molecules are introduced in the unwinding region with the target, therefore, the dual-sensor has the best sensitivity under UV irradiation when 4 PTG molecules are introduced in the unwinding region of promoter (Tables S3 and S4). On the opposite, the dual-sensor has the best sensitivity under the dark when 2 PTG molecules are introduced in the unwinding region (Tables S1 and S2). The results shown in Fig. 3, Fig. 4a, Fig. S4 and Fig. S5a proved that the introduced PTG molecules introduced in the unwinding region completely inhibited the RNAPs to melt the promoters of the indicating genes (indicated by the 0 value of k_{cat}, Fig. 4a, Fig. S5a), due to the integration of the DNA double strands *via* the PTG molecules, hence completely stopped the expression of the indicating genes; whereas, the unwinding region of the promoter will be melt upon very few target arose in the tested system, due to target-induced enlarged DNA bubble. These results also demonstrated the accuracy of the dual-sensor at the aspect of detecting target, it benefits from the ingenious structure of the PTG molecular, which could bind two DNA strands tightly without target-induced enlarged DNA bubble, and could lead to the separation of the two DNA strands undestructively *via* the target-induced enlarged DNA bubble.

3.3. Effect of the introduction of PTG molecules in the recognition region on dual-sensor

Moreover, it was found that under UV irradiation, the additional introduction of *cis*-PTG molecules in the recognition region could facilitate the recognition and binding of RNAPs to the promoter, indicated by the smaller K_m value, as the *cis*-PTG molecules could force

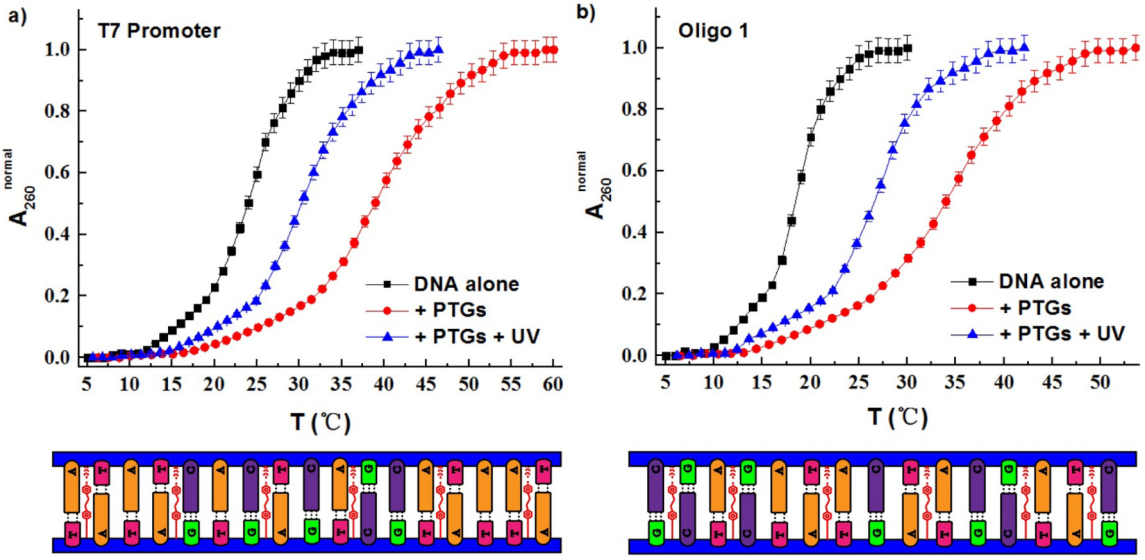

Fig. 2. Melting curves of DNAs. 40.0 μM T7-promoter (a) and 40.0 μM oligo 1 (b) in 10 mMTris buffer (pH = 7). Square: DNA alone; Circle: 6 PTG molecules introduced in the DNAs under the dark condition; Triangle: 6 PTG molecules introduced in the DNAs under UV irradiation at 365 nm.

Fig. 3. Effectiveness of the proposed dual-sensor under UV irradiation at 356 nm. The dual-sensor operates effectively when the number of PTGs introduced in the unwinding region is 4 or and 5.

the sequences of the recognition region to flip out for the easier recognition and binding by RNAPs (Fig. 5a, c, Tables S3 and S4) (Liu et al., 2006). Therefore, the sensitivity of the dual-sensor under UV irradiation can be improved by introducing PTG molecules in the recognition region of the T7 promoter (Fig. S6), and the kinetic study in Fig. 5a, c demonstrated that optimum number of PTG molecules introduced in the recognition region under UV irradiation at 365 nm is 5 in terms of the sensitivity of the dual-sensor. On the opposite, under the dark condition, the introduction of *trans*-PTG molecules into the recognition region have no effect on RNAPs to recognize the promoter at the cases without the target, even have a negative effect at the cases with the presence of target as the formation of the enlarged DNA bubble would be affected (Fig. 5a, b). Therefore, the dual-sensor with 4 PTG molecules introduced in the unwinding region and 5 PTG molecules in the unwinding region (denoted as the smallest value of K_m and the largest value of k_{cat}) would attain the best sensitivity under UV irradiation at 365 nm, whose performance to detect the target nucleic acid and/or chemical molecule was investigated in the next section exampled by Oligo 2 (5′-ATTCGCGATCATCGAGA-3′) and thrombin.

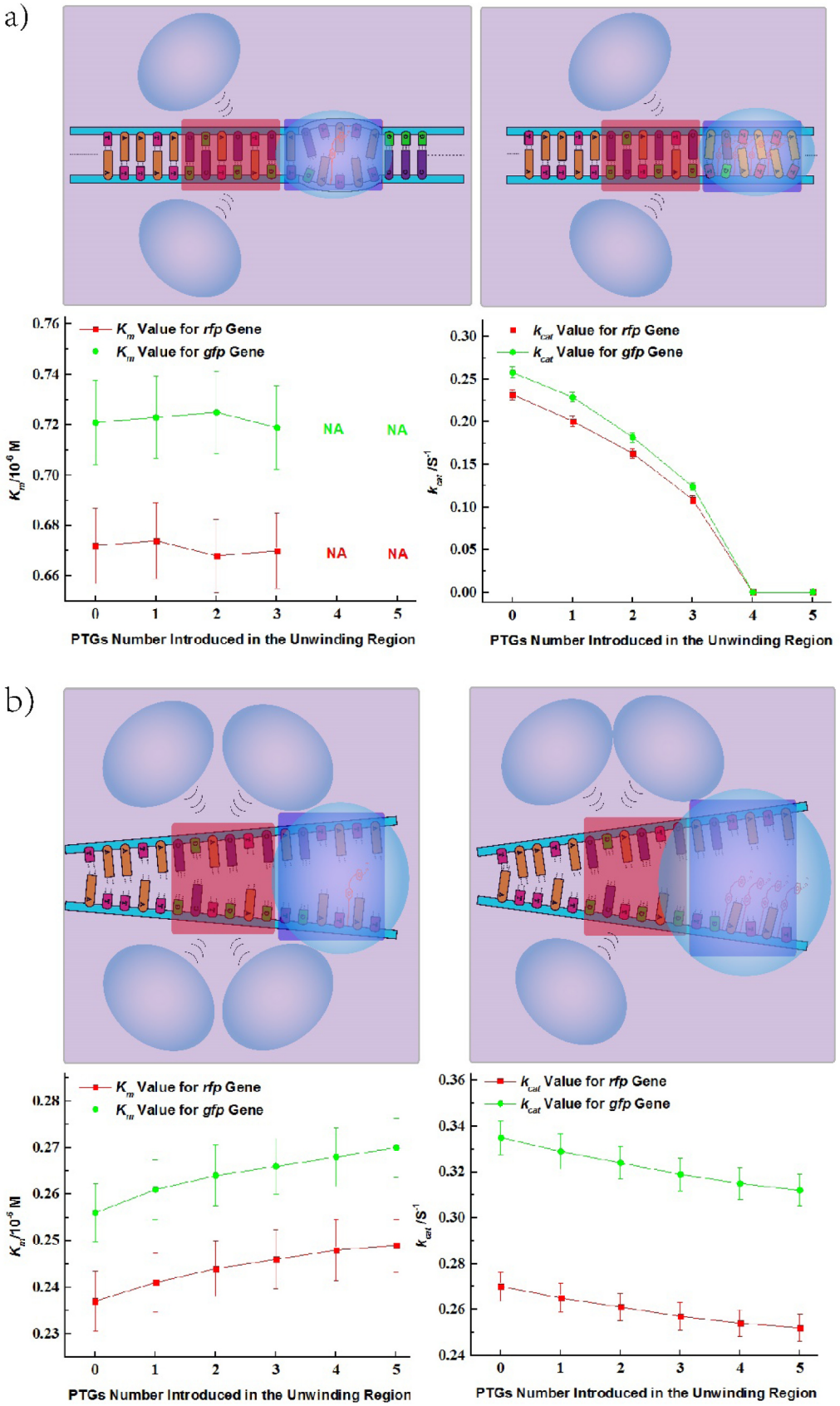

Fig. 4. Effect of the introduction of PTGs in the unwinding region on the RNAPs to recognize and melt the promoter under UV irradiation at 365 nm without (a) or with (b) the target.

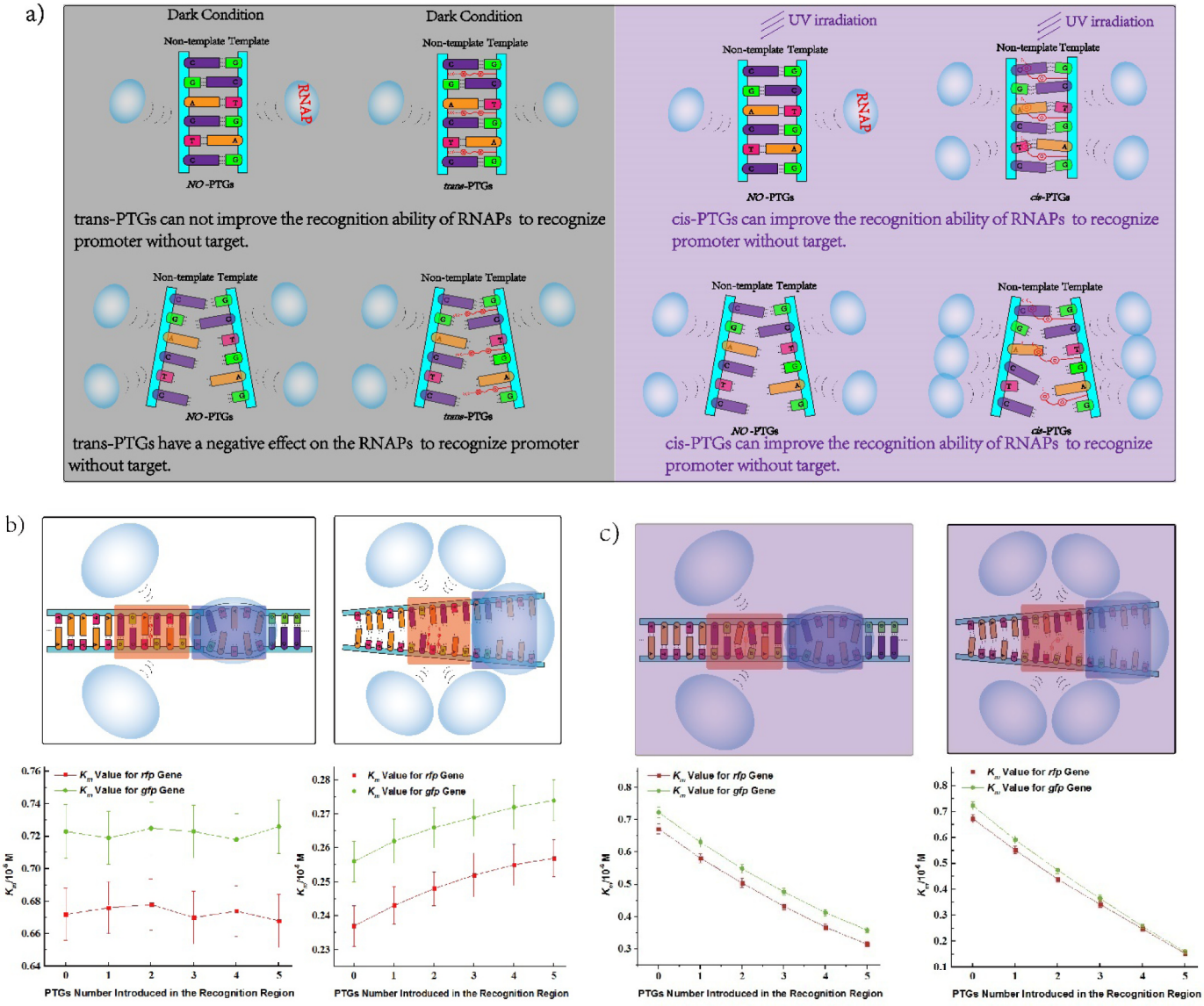

Fig. 5. Effect of the introduction of PTG molecules in the recognition region on the recognition ability of RNAPs to promoter. (a) Different working mechanisms of the dual-sensor under dark condition and UV irradiation; Effect of the introduction of PTG molecules in the recognition region on the recognition ability of RNAPs to promoter under the dark condition without (left) or with (right) the target (b) and under UV irradiation at 365 nm without (left) or with (right) the target (c).

3.4. Quantitative detection of the target utilizing the proposed dual-sensor

The performances of a good detection sensor can be mainly reflected by two indicators: the "high detection sensitivity" with the aim for detecting low concentration of target, as shown in the Fig. 6a-b, on the premise of quantitative of the target, the concentration of thrombin can be detected as low to 0.2 μM (Fig. 6a, about 7.4 ppm) and the concentration of Oligo 2 can be detected as low to 1 μM (Fig. 6b, about 5.4 ppm). Some studies (Yang et al., 2016; Hou et al., 2015; Sun et al., 2015; Liu et al., 2015; Luo et al., 2011) have reported some strategies which could detect target at a relatively low concentration, such as Luo et al. (2011) report a real-time electrochemical monitoring method of amplification of RCR amplicons based on sequence-specific hydrolysis sensor labeled with Fc or MB with a limit of detection down to 0.1 μM; Yang et al. (2016) developed a recyclable electrochemical sensing platform of homogeneous DNA hybridization based on host-guest recognition of pillararenes with a detection range of 0.33 μM to 3.3 nM; Hou et al. (2015) designed a highly sensitive homogeneous electrochemical biosensing strategy with a range from 0.1 to 50 nM based on the split aptamer-incorporated DNA three-way junction and Exo III-assisted target recycling. However, all these sensors cannot quantitative detection of the target, and not flexible enough as only detecting one specific kind of target, what's more, most these sensors are based on cost- and complexed- signal enhancement strategies, while our dual-sensor just need the readout modes. Combing more and more advanced signal enhancement technology, our strategy can provide high potential value for biosensors to detect targets at a very low concentration. The other indicator is the "high detection efficiency", aiming for a stronger signal within a shorter time (Baker et al., 2006), *e.g.*, for the aptamer-based sensor, the amounts of aptamers that changes their conformation in a unit of time when the target is detected (Stojanovic et al., 2001; Yang et al., 2014; Huizenga and Szostak, 1995), in this study, the value of K_m and $\frac{k_{cat}}{K_m}/10^6$ M^{-1} S^{-1} can be used to characterize the "detection efficiency" of the developed dual-sensor as a smaller K_m value and a larger $\frac{k_{cat}}{K_m}/10^6$ M^{-1} S^{-1} value signifying an efficient expression of the indicating genes due to the stronger recognition of RNAP to the promoter and faster speed of RNAP to unwind the promoter. For the conventional gene expression, the $K_m/10^{-6}$ M value is usually ranging between 0.30 and 4.13, while the $K_m/10^{-6}$ M value for the developed

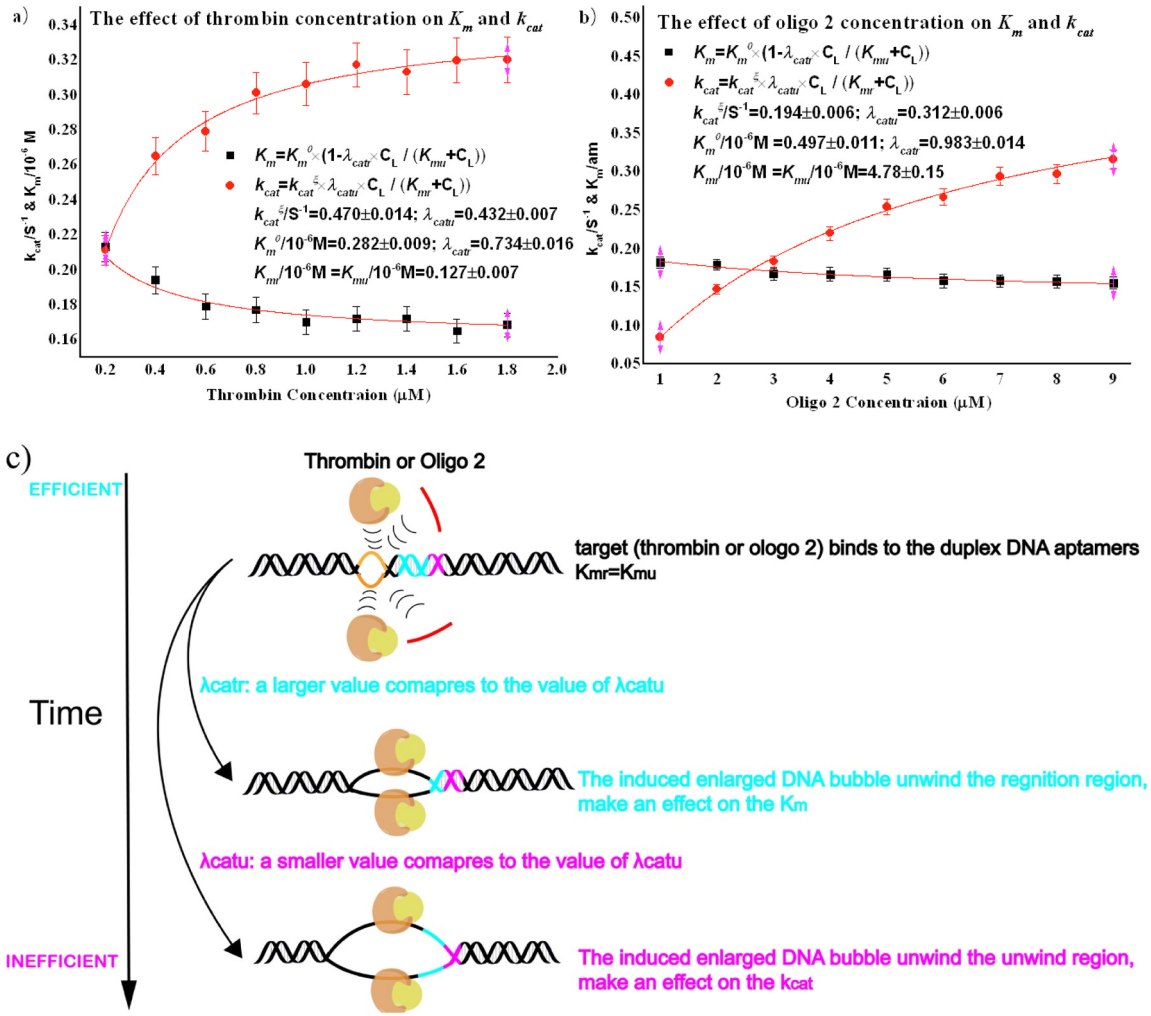

Fig. 6. The effects of the target concentration (thrombin or Oligo 2) on K_m, k_{cat} under T7 RNA polymerase (0.20 μM) for the dual-sensor enclosing *gfp* gene and *rfp* gene (25 ng/μL per reaction). (a) The effects of the thrombin concentration on K_m, k_{cat} for the *gfp* gene; (b) The effects of the thrombin concentration on K_m, k_{cat} for the *gfp* gene; (c) The mechanism of the thrombin with its DNA aptamer on the λ_{catr}, K_{mr}, λ_{catu}, K_{mu}.

dual-sensor with the best sensitivity can reach as small as 0.163 for the *rfp* gene (when the Oligo 2 concentration is 1 μM) and 0.172 for the *gfp* gene (when the thrombin concentration is 1.2 μM); and by referring to the literature (Liu et al., 2006), the value of $\frac{k_{cat}}{K_m}/10^6$ M^{-1} S^{-1} for the conventional gene expression under the T7 promoter is usually ranging from 0.053 to 1.1, while the value of $\frac{k_{cat}}{K_m}/10^6$ M^{-1} $S^{-1}$of the dual-sensor is 1.53 for the *rfp* gene (when the Oligo 2 concentration is 1 μM) and 1.81 for the *gfp* gene (when the thrombin concentration is 1.2 μM), demonstrating that the indicating gene can be expressed at a very high detection efficiency once the target is detected.

Finally, the last but no least advantage of the developed dual-tensor is that it can fulfill the quantitative detection of the target nucleic acid and chemical molecule *via* the GFP/RFP concentration encoded by the *rfp* gene *gfp* gene, and target concentration $C_l = \frac{K_{mr}\cdot C_f\cdot(K_m^0+[S])}{C_f\cdot K_m^0\cdot(\lambda_{catr}-1)+k_{cat}^{\xi}\cdot\lambda_{catu}\cdot E\cdot[S]\cdot\varphi-C_f\cdot[S]}$, and the derivation process is as follows:

According to the Michaelis-Menten plots of transcription rate *versus* concentration of T7 promoter and our previous studies (McClure, 1985; Martin and Coleman, 1987), the ATP (Adenosine triphosphate) incorporation v can be given by:

$$v = \frac{k_{cat}\cdot E\cdot[S]}{K_m + [S]} \tag{1}$$

where E is the RNA polymerase concentration and $[S]$ is the T7 promoter concentration. As the enlarged DNA bubble promotes the transcription rate (Wang et al., 2017a), the k_{cat} and K_m can be given by:

$$k_{cat} = k_{cat}^{\xi}\cdot\frac{\lambda_{catu}\cdot C_l}{K_{mu}+C_l} \tag{2}$$

$$K_m = K_m^0\cdot\left(1-\frac{\lambda_{catr}\cdot C_l}{K_{mr}+C_l}\right) \tag{3}$$

where λ_{catr} is the response rate of the enlarged DNA bubble containing the recognition region; λ_{catu} is the response rate of the enlarged DNA bubble containing the unwinding region; K_{mr} & K_{mu} both are the adsorption efficiency between the target and the DNA aptamer. Combing Eq. (1), Eq. (2) and Eq. (3), the ATP incorporation v can be given by:

$$v = \frac{k_{cat}^{\xi}\cdot\frac{\lambda_{catu}\cdot C_l}{K_{mu}+C_l}\cdot E\cdot[S]}{K_m^0\cdot\left(1-\frac{\lambda_{catr}\cdot C_l}{K_{mr}+C_l}\right)+[S]} \tag{4}$$

From a set of data, the single set of the best fit values for λ_{catr}, K_{mr}, λ_{catu}, K_{mu}, K_m^0 and k_{cat}^{ξ} for the *gfp* gene and *rfp* gene were correlated and showed in Fig. 6a-b.

As the GFP/RFP concentration are in proportion to the ATP incorporation rate v, the GFP/RFP concentration C_f can be given by:

$$C_f = \varphi \cdot \frac{k_{cat}^{\xi} \cdot \frac{\lambda_{catu} \cdot C_l}{K_{mu} + C_l} \cdot E \cdot [S]}{K_m^0 \cdot \left(1 - \frac{\lambda_{catr} \cdot C_l}{K_{mr} + C_l}\right) + [S]} \quad (5)$$

where φ is the ration coefficient between GFP/RFG concentration and ATP incorporation rate, and form Eq. (5), the target concentration can be given by:

$$C_l = \frac{K_{mr} \cdot C_f \cdot (K_m^0 + [S])}{C_f \cdot K_m^0 \cdot (\lambda_{catr} - 1) + k_{cat}^{\xi} \cdot \lambda_{catu} \cdot E \cdot [S] \cdot \varphi - C_f \cdot [S]} \quad (6)$$

The model shown in Fig. 6a-b fits well with the results of this study, the value of λ_{catr}/S^{-1} (0.734 for the *gfp* gene and 0.983 for the *rfp* gene) is larger than the value of λ_{catu}/S^{-1} (0.432 for the *gfp* gene and 0.312 for the *rfp* gene) as the recognition region is upstream the unwinding region, therefore, during the formation of the enlarged DNA bubble, the DNA bubble makes an effect on K_m before k_{cat} (Fig. 6c). Both values of K_{mr} and K_{mu} in the two situations (0.127×10^{-6} M for the *gfp* gene and 4.78 am for the *rfp* gene) are equal as same target bound to the ssDNA has the same effect on K_m and k_{cat} (Fig. 6c), demonstrating the accuracy of the dual-sensor at the aspect of quantitating target. It benefits from the ingenious designed DNA bubble containing DNA aptamer, which has a relatively matured thermodynamic research foundation with its ligand (Wang et al., 2017a, 2017b; Neves et al., 2010; Gouda et al., 2003), hence, it's suitable for us to establish an accuracy dynamic model of the proposed dual-sensor.

4. Conclusions

In summary, we have constructed a novel aptamer-based dual-sensor that can be used to cost-effectively and conveniently detect and quantify any nucleic acids and chemicals whose binding aptamers can be found or synthesized with excellent selectivity. The dual-sensor reveals the absence of the target by inhibiting the expression of the indicating *rfp/gfp* genes, and manifests the detection of the target *via* the expression of the corresponding gene. One significant advantage of the developed sensor is that it can detect the target acid and chemical molecule at the same time, therefore, it can distinguish whether the chemical is produced by the test system by verifying the co-existence of the target nucleic acid sequences and chemical molecule, or only due to the contamination by the foreign chemical *via* manifesting the existence of only the target chemical. Therefore, this work may provide a significant advance in the analytical tools for clinical chemistry: rapid, easy operation, homogeneous assays with the simultaneous report of the presence or absence of multiple disease-marker proteins or nucleic acid related to cancers within bodily fluids.

The working mechanism of the developed dual-sensor is based on the regulation of the melting of the T7 promoter, thus the expression of the indicating genes *via* the combined effect of two DNA bubbles that are introduced upstream the two T7 promoters and PTG molecules that are introduced into the unwinding region and recognition region of the double-stranded DNA. The specifically designed PTG molecules form covalent bonds with the three-carbon-atom linker in one strand *via* the threoninol terminal, and interact non-covalently with the other strand. Without the presence of the target, the indicating genes included in the dual-sensor cannot be expressed due to the enhanced affinity between the two DNA stands resulted by the introduced PTG molecules; while with the presence of the target, the enlarged DNA bubble would help the separation of the two DNA stands, resulting in the melting of the promoter DNA and the expression of the corresponding indicating genes. Moreover, the sensitivity of the dual-sensor can be significantly improved under UV irradiation by inducing the *trans-* to *cis-* transformation of the PTG molecules.

Similar sensors can be constructed for detecting two nucleic acids at the same time by introducing two DNA bubbles containing two different ssDNA sequences, which can hybridize with the two target nucleic acids, respectively. Following the same principle, sensors that detect two small chemical molecules at the same time can also be developed when the two DNA bubbles contain two different aptamers that can be bound with the two chemical targets. The approach to control gene expression by regulating the melting of the promoter DNA proposed in this study can also be extended to other bacteriophage or bacterial promoter sequences, allowing to design devices controlling gene expression in a greater dynamic range. Moreover, by utilizing the proposed UV-sensitive PTG molecules, the DNA-based nanoswitches to transport small molecules could be constructed *via* UV-triggered allosteric regulation with the intention to control cellular processes and pathways.

Acknowledgements

This work is financially supported by the National Science Foundation of China, China (21606026, 21776025), Chongqing Science and Technology Commission, China (CSTC2013jcyA0348), the Fundamental Research Funds for the Central Universities, China (106112017CDJXY220005, 106112017CDJXF220009, 106112017CDJPT220001, 106112017CDJQJ228809, 106112017CDJXFLX0014), National Key R & D Program of China, China (2017YFB0603105), and support by China Scholarship Council, China (201506050056).

Declaration of interest statement

The authors declared that they have no conflicts of interest to this work.

Appendix A. Supplementary material

Supplementary data associated with this article can be found in the online version at doi:10.1016/j.bios.2018.12.015.

References

Asanuma, H., Ito, T., Yoshida, T., Liang, X.G., Komiyama, M., 1999a. Angew. Chem. Int. Ed. 38, 2393–2395.
Asanuma, H., Ito, T., Yoshida, T., Liang, X.G., Komiyama, M., 1999b. Angew. Chem. 111, 2547–2549.
Baker, B.R., Lai, R.Y., Wood, M.S., Doctor, E.H., Heeger, A.J., Plaxco, K.W., 2006. J. Am. Chem. Soc. 128, 3138–3139.
Banga, R.J., Chernyak, N., Narayan, S.P., Nguyen, S.T., Mirkin, C.A., 2014. J. Am. Chem. Soc. 136, 9866–9869.
Beharry, A.A., Woolley, G.A., 2011. Chem. Soc. Rev. 40, 4422–4437.
Bergen, A., Rudiuk, S., Morel, M., Le Saux, T., Ihmels, H., Baigl, D., 2016. Nano Lett. 16, 773–780.
Blondeau, P., Segura, M., Peŕez-Fernańdez, R., de Mendoza, J., 2007. Chem. Soc. Rev. 36, 198–210.
Buryakov, I.A., 2004. J. Chromatogr. B 800 (1–2), 75–82.
Cho, E.J., Lee, J.W., Ellington, A.D., 2009. Annu. Rev. Anal. Chem. 2, 241–264.
Despras, E., Sittewelle, M., Pouvelle, C., Delrieu, N., Cordonnier, A.M., Kannouche, P.L., 2016. Nat. Commun. 7, 13326.
Duan, R.X., Zuo, X.L., Wang, S.T., Quan, X.Y., Chen, D.L., Chen, Z.F., Jiang, L., Fan, C.H., Xia, F., 2013. J. Am. Chem. Soc. 135, 4604.
Elghanian, R., Storhoff, J.J., Mucic, R.C., Letsinger, R.L., Mirkin, C.A., 1997. Science 277, 1078.
Gao, A., Lu, N., Wang, Y., Dai, P., Li, T., Gao, X., Fan, C., 2012. Nano Lett. 12, 5262.
Ge, Z., Lin, M., Wang, P., Pei, H., Yan, J., Shi, J., Huang, Q., He, D., Fan, C., Zuo, X., 2014. Anal. Chem. 86, 2124–2130.
Gouda, H., Kuntz, I.D., Case, D.A., Kollman, P.A., 2003. Biopolymers 68, 16–34.
Harcourt, E.M., Kool, E.T., 2012. Nucleic Acids Res. 40, e65.
Hou, T., Li, W., Zhang, L., Li, F., 2015. Analyst 140, 5748–5753.
Huizenga, D.E., Szostak, J.W., 1995. Biochemistry 34, 656–665.
Iyer, S., Doktycz, M.J., 2014. ACS Synth. Biol. 3, 340–346.
Jayasena, S.D., 1999. Clin. Chem. 45, 1628–1650.
Koshiol, J., Wang, E., Zhao, Y.D., Marincola, F., Landi, M.T., 2010. Cancer Epidemiol. Biomark. Prev. 19, 907.
Krishnan, Y., Simmel, F.C., 2011. Angew. Chem. Int. Ed. 50, 3124–3156.
Lee, J.H., Yigit, M.V., Mazumdar, D., Lu, Y., 2010. Adv. Drug Deliv. Rev. 62, 592–605.
Leshkowitz, D., Horn-Saban, S., Parmet, Y., Feldmesser, E., 2013. RNA 19, 527.
Liu, M., Asanuma, H., Komiyama, M., 2006. J. Am. Chem. Soc. 128, 1009–1015.
Liu, X., Li, W., Hou, T., Dong, S., Yu, G., Li, F., 2015. Anal. Chem. 87, 4030–4036.
Luo, X., Xuan, F., Hsing, I., 2011. Electrochem. Commun. 13, 742–745.
Mairal, T., Ozalp, V.C., Lozano, S.,ˊanchez,, P., Mir, M., Katakis, I., O'Sullivan, C.K., 2008. Anal. Bioanal. Chem. 390, 989–1007.

Martin, C.T., Coleman, J.E., 1987. Biochemistry 26, 2690–2696.
McClure, W.R., 1985. Annu. Rev. Biochem. 54, 171–204.
McKeague, M., DeRosa, M.C., 2012. J. Nucleic Acids 748913.
Merino, E., Ribagorda, M., 2012. Beilstein J. Org. Chem. 8, 1071–1090.
Mirkin, C.A., Letsinger, R.L., Mucic, R.C., Storhoff, J.J., 1996. Nature 382, 607.
Mok, W., Li, Y.F., 2008. Sensors 8, 7050–7084.
Munge, B., Liu, G.D., Collins, G., Wang, J., 2005. Anal. Chem. 77, 4662.
Neves, M.A.D., Reinstein, O., Saad, M., Johnson, P.E., 2010. Biophys. Chem. 153, 9–16.
Niemeyer, C.M., 2000. Curr. Opin. Chem. Biol. 4, 609–618.
Niemeyer, C.M., Adler, M., Pignataro, B., Lenhert, S., Gao, S., Chi, L., Fuchs, H., Blohm, D., 1999. Nucleic Acids Res. 27, 4553–4561.
Nykypanchuk, D., Maye, M.M., van der Lelie, D., Gang, O., 2008. Nature 451, 549–552.
Rothemund, P.W.K., 2006. Nature 440, 297–302.
Ruigrok, V.J.B., Levisson, M., Eppink, M.H.M., Smidt, H., van der Oost, J., 2011. Biochem. J. 436, 1–13.
Sacca, B., Niemeyer, C.M., 2012. Angew. Chem. Int. Ed. 51, 58–66.
Seeman, N.C., 2003. Nature 421, 427–431.
Smith, S.J., Nemr, C.R., Kelly, S.O., 2017. J. Am. Chem. Soc. 139 (1020-1-28).
Soleymani, L., Fang, Z., Lam, B., Bin, X., Vasilyeva, E., Ross, A.J., Sargent, E.H., Kelley, S.O., 2011. ACS Nano 5, 3360.
Soleymani, L., Fang, Z., Sargent, E.H., Kelley, S.O., 2009. Nat. Nanotechnol. 4, 844.
Stojanovic, M.N., de Prada, P., Landry, D.W., 2001. J. Am. Chem. Soc. 123, 4928–4931.
Strano-Rossi, S., Molaioni, F., Rossi, F., Botre, F., 2005. Rapid Commun. Mass Spectrom. 19, 1529–1535.
Sun, A., Deng, K., Fu, W., 2015. Biosens. Bioelectron. 74, 66–70.
Tagliaro, F., Antonioli, C., De Battisti, Z., Ghielmi, S., Marigo, M., 1994. J. Chromatogr. A 674 (1–2), 207–215.
Taton, T.A., Mirkin, C.A., Letsinger, R.L., 2000. Science 289, 1757.
Trachta, G., Schwarze, B., Saegmuller, B., Brehm, G., Schneider, S., 2004. J. Mol. Struct. 693 (1–3), 175–185.
VanGuilder, H.D., Vrana, K.E., Freeman, W.M., 2008. BioTechniques 44, 619–626.
Wang, J., Yang, L., Cui, X., Zhang, Zhe, Dong, L., Guan, N., 2017a. ACS Synth. Biol. 6, 758–765.
Wang, J., Cui, X., Yang, L., Zhang, Z., Lv, L., Wang, H., Zhao, Z., Guan, N., Dong, L., Chen, R., 2017b. Metab. Eng. 42, 85–97.
Weisburg, W.G., Barns, S.M., Pelletier, D.A., Lane, D.J., 1991. J. Bacteriol. 173, 697–703.
Wilhelm, J., Pingoud, A., 2003. ChemBioChem 4, 1120–1128.
Yang, K.A., Barbu, M., Halim, M., Pallavi, P., Kim, B., Kolpashchikov, D.M., Pecic, S., Taylor, S., Worgall, T.S., Stojanovic, M.N., 2014. Nat. Chem. 6, 1003–1008.
Yang, S., Liu, L., You, M., Zhang, F., Liao, X., He, P., 2016. Actuators B Chem. 227, 497–503.